Composites Science and Technology 165 (2018) 31–38

Contents lists available at ScienceDirect

Composites Science and Technology

journal homepage: www.elsevier.com/locate/compscitech

Fabrication of a piezoelectric polyvinylidene fluoride/carbonyl iron (PVDF/CI) magnetic composite film towards the magnetic field and deformation bi-sensor

Min Sang[a], Sheng Wang[a], Mei Liu[a], Linfeng Bai[a], Wanquan Jiang[a,*], Shouhu Xuan[b], Xinglong Gong[b,**]

[a] Department of Chemistry, Collaborative Innovation Center of Suzhou Nano Science and Technology, University of Science and Technology of China (USTC), Hefei 230026, PR China

[b] CAS Key Laboratory of Mechanical Behavior and Design of Materials, Department of Modern Mechanics, USTC, Hefei 230027, PR China

ARTICLE INFO

Keywords:
PVDF/CI film
Piezoelectricity
Magneto-electricity
Sensor

ABSTRACT

In this paper, a versatile polyvinylidene fluoride/carbonyl iron (PVDF/CI) composite film was prepared by doping magnetic carbonyl iron (CI) particles into piezoelectric polyvinylidene fluoride (PVDF) matrix. Without influencing the piezoelectric structure of PVDF, CI particles enhanced the Young's modulus and maximum tensile strength of composite films. Due to the magnetic driven characteristic, PVDF/CI composite films exhibited distinct magnetic-mechanic-electric coupling properties. The piezoelectric charge signals could be generated by applying the bending deformation or magnetic field. Taking PVDF/CI-10% (CI content was 10 wt%) film as an example, the piezoelectric charges under 2, 4, 6, 8, and 10 mm bending displacement were 3.0, 9.6, 14.9, 18.6, and 24.6 pC respectively. Moreover, when the magnetic field varied from 0 to 600 mT, the generated magneto-electric charges of PVDF/CI-10% film increased from 0 to 676 pC. The quantitative relationship between magnetic field and magneto-electric charges was obtained by the polynomial fitting method and the correlation coefficient was up to 0.97. Owing to the ideal piezoelectricity, excellent stability, light weight and desirable flexibility, PVDF/CI composite films showed promising applications in deformation sensor and magnetic field sensor.

1. Introduction

Magneto-electric (ME) coupling composite material which is composed of two kinds of single-phase materials, namely, the magnetostrictive phase and the piezoelectric phase, is a new type of functional material with increasing applications in many areas such as flexible electronics and sensors [1,2], microwave absorbing [3,4], energy harvesting [5,6] and electromagnetic interference shielding [7,8]. Magneto-electric (ME) coupling effect [9–12] is an interesting phenomenon whose electric polarization varies under the applied magnetic field or electric field. Typically, magneto-electric materials can be subdivided into two major categories: single-phase magneto-electric materials and magneto-electric composites. Although the firstly discovered magneto-electric materials are single-phase materials (such as Cr_2O_3 and $BiFeO_3$), low working temperature and small magneto-electric effect confine their applications at room temperature. Therefore, magneto-electric composite materials become attractive on account of their strong magneto-electric effect at room temperature.

Polyvinylidene fluoride (PVDF) is the most commonly used piezoelectric polymer which possesses five distinct crystalline phases named as α, β, γ, δ, and ε [13]. The β-phase of PVDF matrix shows the strongest piezoelectric response and is considered as the main piezoelectric phase. Due to their high piezoelectric coefficient, excellent stability and desirable flexibility, PVDF polymer-based composites have attracted increasing interests [14–19]. Owing to the magnetic driven property, the representative magneto-electric composites could be achieved by adding magnetic particles into PVDF matrix. To our knowledge, only a few works were devoted to magnetic PVDF polymer-based composites and investigated their magneto-electric coupling characteristics. Fang et al. [20] developed a three-layered multiferroic composite by sandwiching one P(VDF-TrFE) layer between the two conductive layers of CFO($CoFe_2O_4$)-CNT-PVDF. The magnetoelectric coupling of composite increased with the volume fraction of CFO nanoparticles. The results offered a guideline for selecting proper

* Corresponding author.
** Corresponding author.
E-mail addresses: jiangwq@ustc.edu.cn (W. Jiang), gongxl@ustc.edu.cn (X. Gong).

https://doi.org/10.1016/j.compscitech.2018.06.006
Received 12 March 2018; Received in revised form 1 June 2018; Accepted 5 June 2018
Available online 15 June 2018

magnetoelectric composites on specified device applications. Unfortunately, the above magneto-electric behavior was weak due to the small magnetic property of doped particles.

The magneto-electric behavior plays a key role in determining the sensing performance of magneto-electric composites in magnetic field sensor. During the past decade, researchers have developed several magnetic field sensors [21,22] using different physical, chemical or biological effects. Reis et al. [23] reported a $Fe_{61.6}Co_{16.4}Si_{10.8}B_{11.2}$ (FCSB)/PVDF/FCSB magneto-electric laminates which could be used as a magnetic field sensor. However, it only sensed the magnetic field between 0 and 5 Oe, which was not suitable for the high magnetic field. Therefore, the high magnetic saturation is highly desired for magnetic PVDF polymer-based composites because the magnetic driven property is originated from magnetic particles. Carbonyl iron (CI) particle is a metallic magnetic powder which exhibits soft magnetic properties. Due to its large saturation magnetization, high permeability, and superior thermal stability, the magnetic CI particle becomes a good choice for magnetic PVDF polymer-based composites [24,25]. To this end, the demand for PVDF/CI composites towards the deformation and magnetic field bi-sensor inspired our present research.

In this work, we reported a novel magneto-electric composite film towards the deformation sensor and magnetic field sensor by dispersing magnetic CI particles into piezoelectric PVDF matrix through a solution-casting process. The β-phase PVDF film was obtained through crystallization from the solution under high temperature, thus PVDF/CI composites exhibited the piezoelectricity. Then, mechanic-electric coupling properties were studied with unilateral bending experiments, which suggested that PVDF/CI composite films possess distinct piezoelectric effect under the stimulation of different deformations. The bending experiments under the loading of magnetic field between 0 and 600 mT were further carried out and the quantitative relationship between magnetic field and magneto-electric charges was eventually discussed. Finally, PVDF/CI composite is expected to be widely applied in sensing the deformation and magnetic field.

2. Material and experiments

2.1. Materials

Poly(vinylidene fluoride) (PVDF) pellets were purchased from Sigma-Aldrich and *N*-methyl pyrrolidone (NMP) was provided by Aladdin chemical Co., Ltd. The magnetic carbonyl iron particles (type CN with an iron content greater than 99.5%) with an average size of 5 μm were purchased from BASF in Germany. Polydimethylsiloxane (PDMS) precursor and curing agent (Sylgard 184) used as packaging and protective material were provided by Dow Corning.

2.2. Fabrication of magneto-electric PVDF/CI composite films

PVDF/CI magnetic films were synthesized by the solution-casting process. 10.6 g PVDF pellets were dissolved in 60 mL NMP at 60 °C with magnetic stirring in the oil bath for 2 h to prepare the PVDF stock solution. Subsequently, different weight ratios of CI particles were added into PVDF solution and mechanically stirred in the water bath at 60 °C for 2 h. In this work, the weight content of CI particles varied from 0 to 1, 5, 10 wt%. After that, each solution was cast onto a clean and horizontal glass plate in a vacuum oven, evaporated at 80 °C for 12 h and annealed at 120 °C for 8 h [26]. Then, through the magnetic sputtering method, upper and lower surfaces of the film were coated with gold films used as electrodes. To protect gold films from falling off, PDMS was used as packaging material and PVDF/CI magneto-electric composite films were finally obtained (Fig. 1). For simplicity, films were named as PVDF, PVDF/CI-1%, PVDF/CI-5%, and PVDF/CI-10% with 0, 1, 5, and 10 wt% of CI fillers, respectively. Besides, the each layer thickness of PVDF/CI film is investigated by the SEM image of cross-section structure of PVDF/CI-10% composite (Fig. SI1).

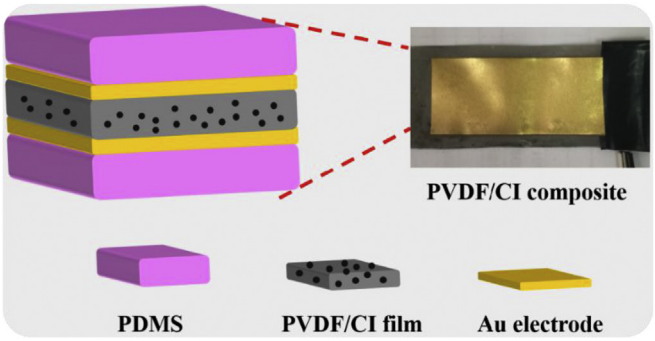

Fig. 1. A schematic diagram of PVDF/CI composite structure shows five layers: the piezoelectric PVDF/CI layer, top/bottom Au electrodes, and top/bottom PDMS packaging layers. The inset shows a digital image of PVDF/CI composite film.

2.3. Characterization

The surface morphology of PVDF film was observed by Scanning Electron Microscopy (SIRION200) and the cross-sectional topography of PVDF film was observed by Environmental Scanning Electron Microscopy (XL-30 ESEM). The crystalline phases of PVDF film were identified by X-ray diffraction (XRD) (SmartLab™ 9 kW, Japan) and Fourier Transform Infrared Spectroscopy (FTIR) technique in a Bruker alpha apparatus in ATR mode from 4000 to 400 cm^{-1} using 24 scans at a resolution of 4 cm^{-1}. The thermal behavior of PVDF film was evaluated by Differential Scanning Calorimetry (DSCQ2000) and the thermal stability was examined by ThermoGravimetric analysis (TGA Q5000IR). The hysteresis loop of CI particles and PVDF/CI film were measured by HyMDC (Hysteresis Measurement of Soft and Hard Magnetic Materials). The tensile properties of PVDF films were examined by the Material Test System (MTS). The gold electrode coating process was accomplished by the magnetic sputtering station (SP-2). In this work, the piezoelectric charges of PVDF films were measured according to the assembled devices in the laboratory (Fig. SI2).

3. Results and discussion

3.1. Characterization of PVDF/CI composite films

The scanning electron microscopy (SEM) is employed to observe the surface morphology of PVDF and PVDF/CI films. As plotted in Fig. 2a, CI particles show a typically spherical shape with an average size about 4 μm. Without CI particles, it is observed that the surface of PVDF film is very smooth and no other impurity is found (Fig. 2b). After doping CI particles into PVDF matrix, the surface of PVDF matrix becomes a little rough and CI particles are obviously distributed on the surface of the film (Fig. 2c and d). Visibly, CI particles are uniformly dispersed in PVDF matrix (Fig. 2e–h). With increasing of the CI content, the density increases.

The cross-section morphology of PVDF and PVDF/CI films is observed by environmental scanning electron microscope (ESEM). As shown in Fig. 2i–l, CI particles are well encapsulated by PVDF matrix, which indicates that magnetic CI particles are successfully doped into PVDF film. Additionally, it is measured that the thickness of PVDF, PVDF/CI-1%, PVDF/CI-5%, and PVDF/CI-10% films is approximately 54, 45, 48, and 58 μm, respectively. Because the cut face of each film is not very flat, the thickness of each sample has a certain difference.

XRD measurements are carried out to examine the crystalline phase of PVDF and PVDF/CI films. As seen from Fig. 3a, the peak at 18.4° corresponds to the α-phase and the peak at 20.2° corresponds to the β-phase. Clearly, it is concluded that CI particles exhibit few negative effects on the phase formation of PVDF matrix. It is commonly known that PVDF is a radically piezoelectric polymer which possesses five

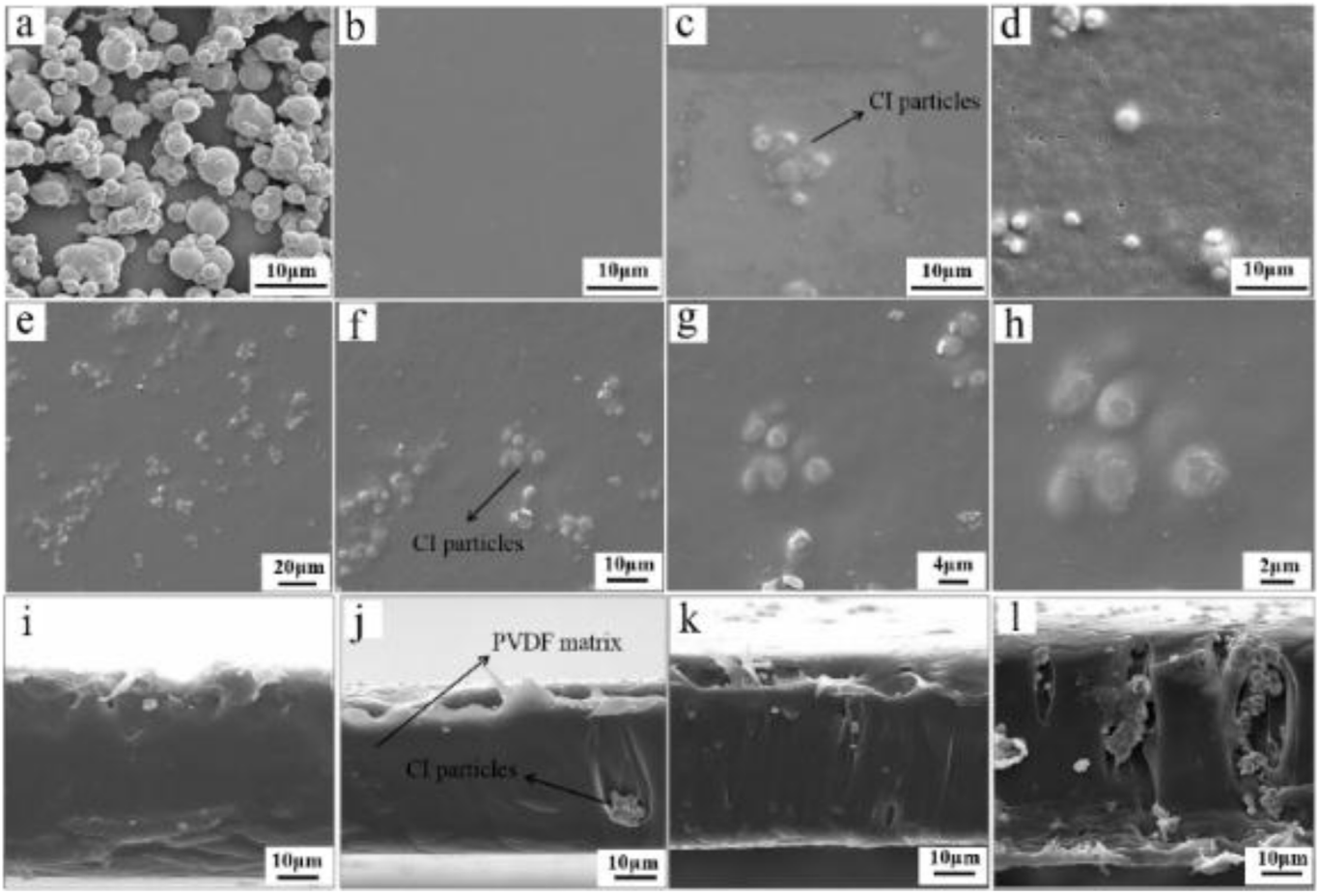

Fig. 2. The surface morphology of (a) CI particles, (b) PVDF, (c) PVDF/CI-1%, (d) PVDF/CI-10% films and PVDF/CI-5% film at different magnifications of (e) 500X, (f) 1000X, (g) 2000X and (h) 4000X. The cross-section morphology of (i) PVDF, (j) PVDF/CI-1%, (k) PVDF/CI-5% and (l) PVDF/CI-10% films.

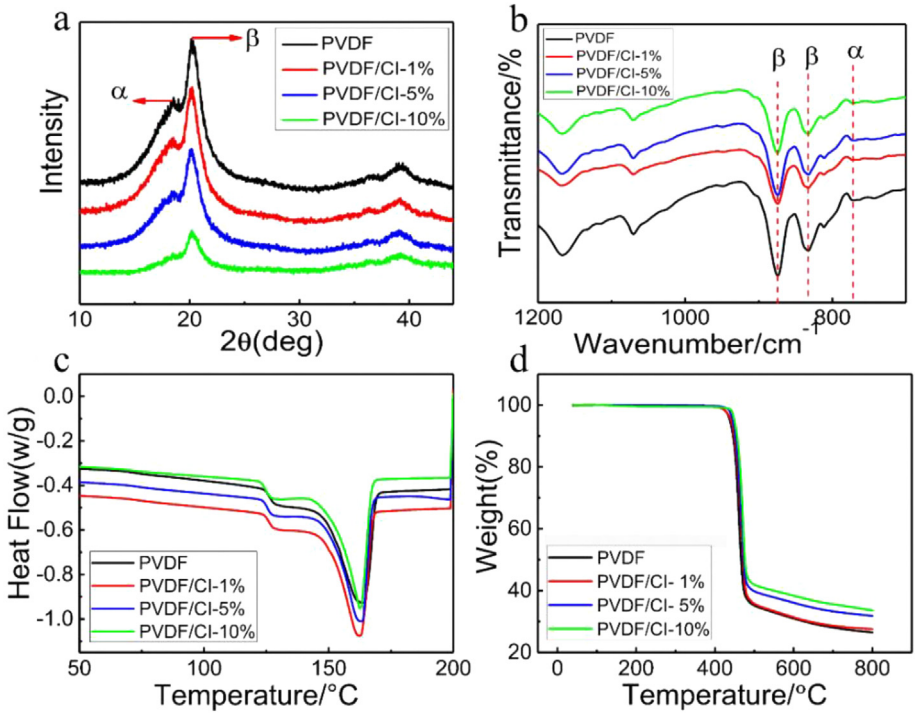

Fig. 3. (a) The XRD pattern, (b) the FTIR spectrum, (c) DSC melting endotherms and (d) TGA curves of PVDF and PVDF/CI films.

distinct α, β, γ, δ, and ε crystalline phases [13]. In particular, the β-phase of PVDF matrix showing the strongest piezoelectric response is considered as the main piezoelectric phase. The XRD results clarify that all the PVDF/CI films with different CI contents contain piezoelectric β-phase, thus they will be expected for showing the piezoelectricity. Fig. 3b shows the FTIR spectrum of PVDF and PVDF/CI films in the range of 1600–700 cm^{-1}. The α-phase is observed at 772 cm^{-1} and the β-phase is located at 833 and 875 cm^{-1}. Besides, the β-phase content ($F(\beta)$) of PVDF/CI composite with different CI contents is calculated in the supplementary information [27] (Fig. SI3a). With different CI contents, the variation of β-phase content is small. The FTIR analysis reveals that solution-casted films mainly contain β-phase and the CI particle shows few effects on the formation of phase. Remarkably, FTIR test result is in accordance with XRD experimental result.

DSC measurements are carried out to explore the crystalline behavior of PVDF and PVDF/CI films. The melting endotherms (Fig. 3c) and crystallization exotherms (Fig. SI4) are presented. Approximately, all the four samples exhibit a melting peak at 160 °C and a crystallization peak at 130 °C. Without affecting the formation of crystal phases, CI particles also do not alter the melting and crystallization temperature of PVDF/CI films. Besides, the crystallinity content (X_C) of PVDF/CI composite is figured out in Fig. SI3b [27], showing the degree of crystallinity is not influenced by the CI content. Consequently, the crystalline structure of PVDF/CI film is not destroyed by CI particles. This result is consistent with both the FTIR and XRD analysis.

The influence of CI particles on the thermal stability of PVDF matrix is investigated by TGA analysis. Fig. 3d plots the thermal decomposition curves of PVDF and PVDF/CI films. The mass of carbonyl iron particles basically remains constant during the TGA test between 40 and 800 °C, revealing that CI particles have good thermal stability at high temperature (Fig. SI5a). For PVDF films, only one degradation step is observed in the measured temperature range (Fig. 3d). By taking differential of TG curves, the maximum thermal degradation temperature of PVDF films can be obtained (Fig. SI5b). For PVDF film, the decomposition process happens at about 460 °C and the weight loss is approximately 62%. As we know, the theoretical content of hydrogen and fluorine in PVDF matrix is 62.4%, thus the decomposition process at 460 °C is attributed to the decomposition of hydrogen fluoride and the residue is carbon. After adding CI particles into PVDF matrix, the final residual components of PVDF, PVDF/CI-1%, PVDF/CI-5%, and PVDF/CI-10% films are 26.5, 27.6, 31.4, and 35.6 wt% respectively, which agree that the content of CI particles are approximately 0, 1, 5, and 9 wt % in PVDF, PVDF/CI-1%, PVDF/CI-5%, and PVDF/CI-10% films, respectively. Compared with PVDF film, no small shift in DTG curve (Fig. SI5b) is found, suggesting that the thermal stability of PVDF/CI film is similar to PVDF matrix. Therefore, it is concluded that CI fillers perform no effect on the thermal stability of PVDF matrix.

3.2. The tensile properties of PVDF/CI composite films

Fig. 4b shows the representative tensile properties of as-prepared PVDF films. During the tests, the rate of uniaxial tensile is set as 1 mm/min. It is found that the stress-strain curves of PVDF and PVDF/CI films exhibit significant yielding and strain hardening. When the applied strain is smaller than 2%, the change of tensile stress for all the 4 samples is nearly linear. Then, they go through a plastic stage before finally being fractured. The maximum tensile strength of PVDF/CI-1%, PVDF/CI-5% and PVDF/CI-10% films are 44.2, 47.7 and 49.5 MPa, respectively, which are larger than PVDF film (43.6 MPa). In comparison to the PVDF film (1.6 GPa), the PVDF/CI-1% (1.8 GPa), PVDF/CI-5% (2.1 GPa) and PVDF/CI-10% (2.2 GPa) films exhibit larger Young's moduli in the elastic stage. Therefore, the CI particles improve both maximum tensile strength and Young's moduli of PVDF matrix. However, the pure PVDF film shows a higher elongation at fracture than PVDF/CI composite films, indicating a decreased elasticity.

3.3. The magnetic properties of PVDF/CI composite films

The magnetic property plays an essential role in determining magnetic-mechanic-electric coupling properties of PVDF/CI films, the intrinsic magnetic responsive properties of PVDF/CI films are investigated by HyMDC at room temperature (Fig. SI6). Fig. 5 exhibits the *M-H* curves of CI particles and PVDF/CI films. Since CI particles are magnetic, they could be magnetized and saturated in the magnetic field. With the increase of magnetic field, the magnetization also increases and eventually saturates. The saturation magnetization (*Ms*) of CI particles are 227 emu/g. The magnetization curve is essentially coincident with the demagnetization one, which exhibits typical soft magnetic properties. Because the magnetic characteristic of PVDF/CI composite is solely originated from magnetic CI particles, PVDF/CI composite exhibits similar magnetic properties to CI particles and could also be magnetized and saturated in the magnetic field. Moreover, with increasing of CI content in PVDF/CI composite, the magnetic moment vector of the magnetic dipole in unit volume also increases, thus resulting in higher magnetization and continuous increase in saturation magnetization of composites. The *Ms* for PVDF/CI-1%, PVDF/CI-5% and PVDF/CI-10% films are 18, 20 and 29 emu/g respectively (Fig. 5b). Due to the high *Ms* of CI particles, PVDF/CI composites are responsive to the stimuli of the magnetic field. To this end, PVDF/CI composites possess broad potential in the magnetic field sensor.

3.4. The unilateral bending test of PVDF/CI composite films towards a deformation sensor

The unilateral bending test device of composite films is set up by MTS to analyze their mechanical-electric coupling properties (Fig. 6a).

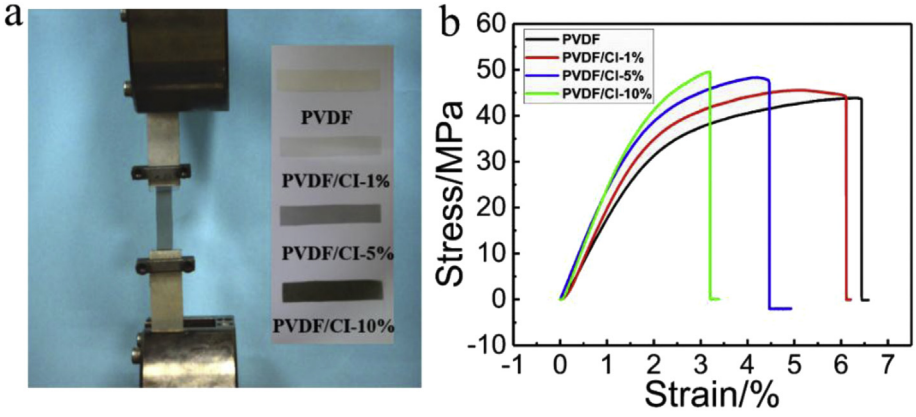

Fig. 4. (a) Experimental device of uniaxial tensile measurement using MTS. (b) Tensile stress-strain curves of PVDF and PVDF/CI films.

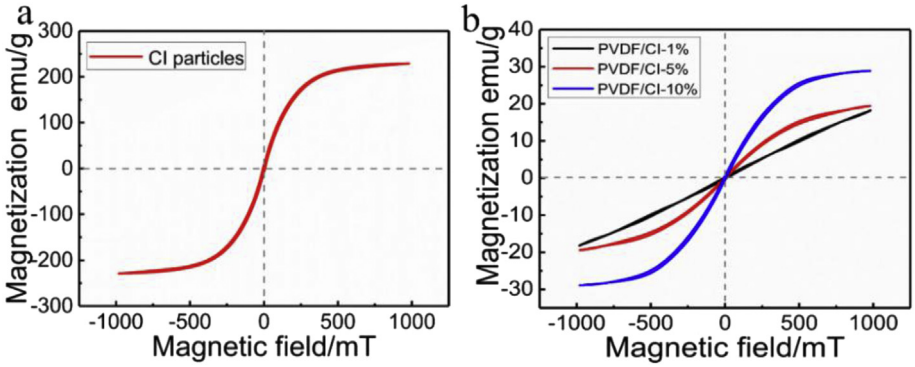

Fig. 5. The magnetic hysteresis loops of (a) CI particles and (b) PVDF/CI films.

The value of the mechanical force required for the bending of the sample is too small to be recorded by the present MTS (Fig. SI7), thus we explore the deformation dependent piezoelectric behavior of PVDF/CI composite. As we know, PVDF matrix exhibits distinct piezoelectric properties, once PVDF films are subjected to the bending deformation, the film will simultaneously produce piezoelectric charges. This phenomenon is called the positive piezoelectric effect of piezoelectric materials [28,29]. As shown in Fig. 6b, when the bending displacement is applied, the piezoelectric charge is generated and it increases with the bending displacement. Since CI particles hardly affect the

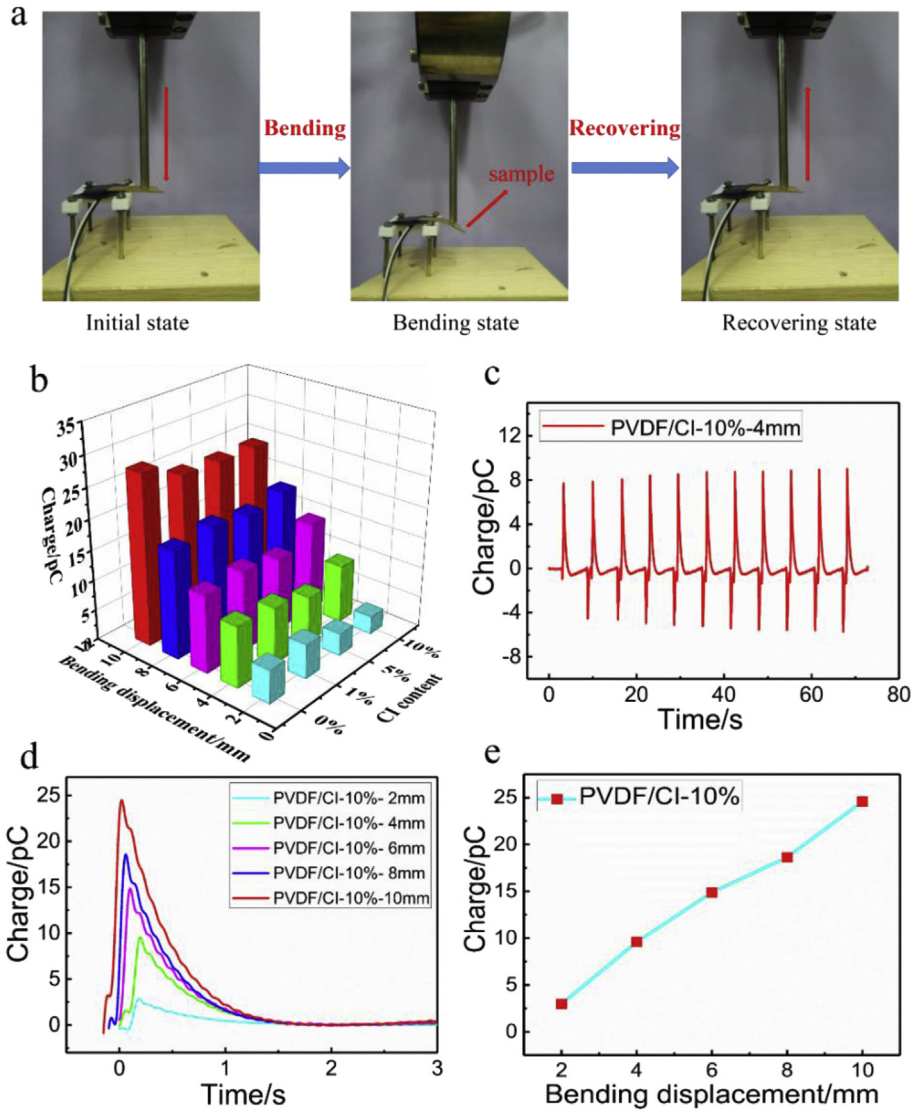

Fig. 6. (a) Schematic diagram of unilateral bending experiment measurement using MTS test device (the effective bending length of the sample is 3 cm), (b) the piezoelectric charges of four samples under different bending displacements, (c) the cyclic unilateral bending tests under 4 mm bending displacement of PVDF/CI-10% film, (d) and (e) the different piezoelectric charges of PVDF/CI-10% film under 2, 4, 6, 8, and 10 mm bending displacement respectively.

piezoelectric structure of β-phase PVDF matrix, the generated piezoelectric charges under the same bending displacement are free from influence of the CI content. Therefore, all the PVDF and PVDF/CI films display the deformation dependent piezoelectric behavior. For PVDF/CI-10% film, it is tested that the piezoelectric charges under 2, 4, 6, 8, and 10 mm bending displacement are 3.0, 9.6, 14.9, 18.6, and 24.6 pC respectively (Fig. 6d and e). Obviously, the piezoelectric signals increase with the augment of bending deformation, revealing that PVDF composite films can be widely applied in the field of sensing, as a means of measuring the deformation of materials. Moreover, the piezoelectric charges of PVDF/CI-10% film under 4 mm bending displacement are basically consistent during 11 cyclic experiments (Fig. 6c), indicating its excellent practicability and stability. In conclusion, PVDF/CI films can generate piezoelectric signals under different deformations, and the ideal cyclic stability guarantees composite films could be further applied in deformation or force sensor.

3.5. The unilateral bending test of PVDF/CI composite films under the loading of magnetic field towards a magnetic field sensor

Based on the above unilateral bending test results, it is noted that PVDF/CI films show distinguished piezoelectric properties under the external stimulation. Since PVDF/CI films are responsive to the external magnetic field, they will also be extended for the magnetic field sensor. Firstly, the magnetic-mechanic-electric coupling properties of PVDF/CI films under the loading of magnetic field are evaluated. Fig. 7a shows the simplified schematic diagram of unilateral bending test under the loading of magnetic field. A rheometer with a permeable framework is used to generate magnetic field and the magnetic flux density ranging from 0 to 600 mT is achieved by adjusting the electromagnetic coil current from 0 to 4.8 A (Fig. SI8). Fig. 7b shows the digital images of bending deformation of PVDF/CI films under the loading/unloading of magnetic field. In the initial state, the composite film remains flat. When the magnetic field is applied, the composite film bends under the action of magnetic force. After unloading the magnetic field, the composite film comes back to its initial state. The result suggests that PVDF/CI films exhibit a quick and timely response to the external magnetic field.

Fig. 7c plots the magneto-electric charges of PVDF films under various magnetic field loading from 0 to 600 mT. Apparently, magneto-electric charges increase with the magnetic field loading and the content of CI particles, indicating that all the PVDF/CI magnetic films possess good magnetic-mechanic-electric coupling properties under applying the magnetic field. Besides, it is highlighted that PVDF film almost has no charge signal under the external magnetic field, because of the insensitivity of PVDF matrix to magnetic field. According to Fig. 7c, it is accepted that PVDF/CI-10% film exhibits the strongest magneto-electric property. The magneto-electric charges of PVDF/CI-10% film increase from 0 to 676 pC when the magnetic field loading increases from 0 to 600 mT, revealing good magnetic driven performance at the presence of magnetic field (Fig. 7e). In details, when applying 0, 100, 200, 300, 400, 500, and 600 mT magnetic field, the generated magneto-electric charges are 0, 50, 192, 358, 525, 603, and 676 pC, respectively. The magnetic-mechanic-electric coupling properties of PVDF/CI-1% and PVDF/CI-5% films are also presented (Fig. SI9).

The quantitative relationship between magnetic field and magneto-electric charges of PVDF/CI-10% film is further figured out by the polynomial fitting method. Fig. 7f shows the polynomial fitting curve and it is calculated that the magnetic flux density and magneto-electric charge signals satisfy the polynomial formula followed as below:

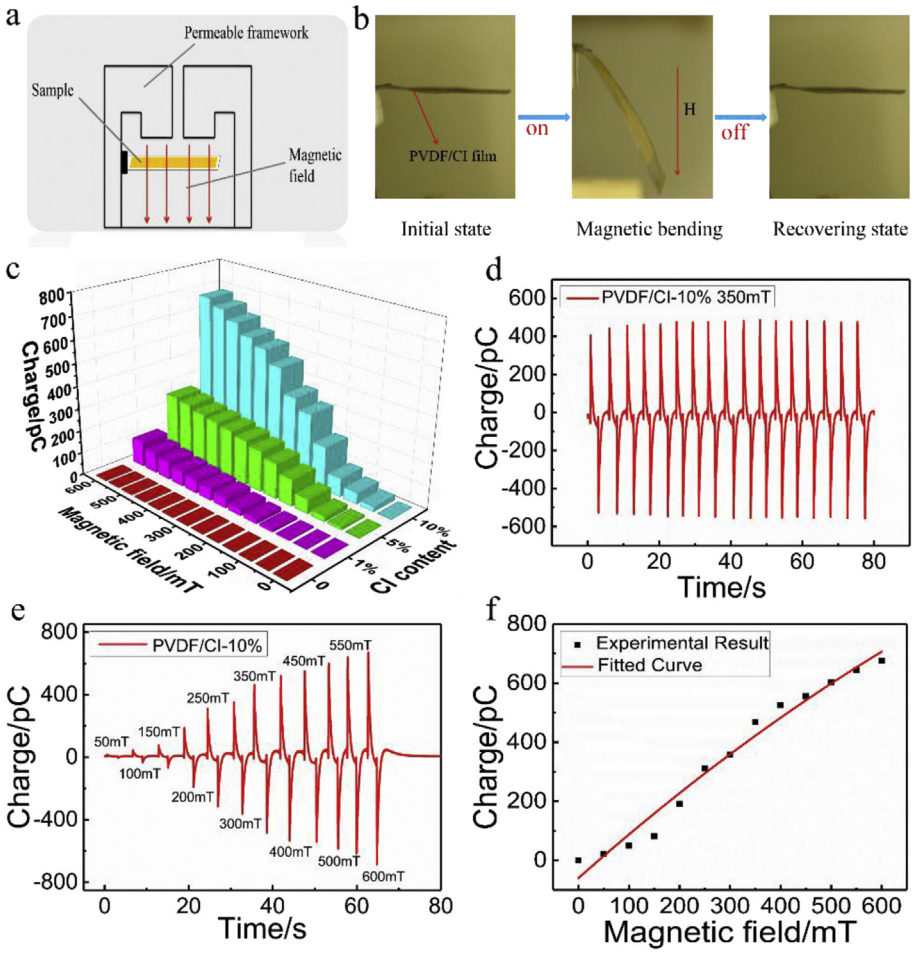

Fig. 7. (a) The simplified schematic diagram of unilateral bending test under the loading of magnetic field generated by a rheometer with a permeable framework. (b) The digital images of bending deformation of PVDF/CI films under the loading/unloading of magnetic field. (c) The magneto-electric charges of four samples under different loading of magnetic field between 0 and 600 mT. (d) The 17 cyclic unilateral bending experiments of PVDF/CI-10% film under 350 mT magnetic field loading. (e) The various magneto-electric charges produced by PVDF/CI-10% magnetic film under different loading of magnetic field from 0 to 600 mT. (f) The quantitative relationship between magnetic field and magneto-electric charges of PVDF/CI-10% film by the polynomial fitting method.

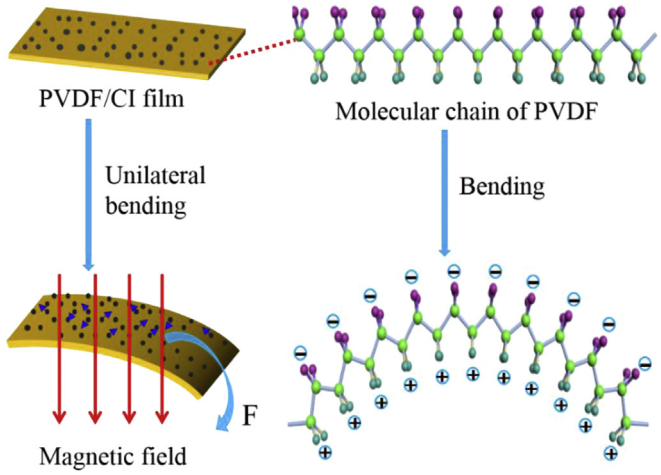

Fig. 8. Schematic illustration of the mechanism of magnetic-mechanic-electric coupling properties.

$$Y = -3.99*10^{-4}X^2 + 1.52X - 59.95$$

Where X represents the different magnetic flux density, and Y represents the number of magneto-electric charges generated by PVDF/CI magnetic films. Furthermore, the correlation coefficient of polynomial fitting is up to 0.97, revealing a good agreement between the fitting curve and experimental data. For instance, if PVDF/CI-10% film generates 468 pC magneto-electric charges, it can be calculated that the applied magnetic field is approximately 350 mT. This result suggests a promising application of PVDF/CI film in the magnetic field sensor. Besides, it can be observed a sudden change in the behavior after initial low slope (Fig. 7f). According to the magnetic hysteresis loop of PVDF/CI composite (Fig. 5b), when the magnetic field is low, the magnetic susceptibility of the material is higher, the magnetostrictive effect is more obvious. With the increase of the magnetic field, the magnetic susceptibility becomes smaller, the magnetic property of composite is weakened, and the magnetostrictive effect is reduced. This may cause initial high slope. For another hand, the magnetic field force is small in the low magnetic field, thus the deformation of PVDF/CI film is small, and its sensitivity to magnetic field is low. When the magnetic field increases, the magnetic field force increases, which forces the PVDF/CI film to deform more obviously, thus the composite is more sensitive to magnetic field. Therefore, the initial slope is low. Based on the above analysis, it can be concluded that the sudden change in the behavior after initial low slope may be caused by small initial magnetic induced force at low magnetic field.

To further investigate the practicability and stability of PVDF/CI films, recycling experiments of PVDF/CI-10% film under 350 mT magnetic field loading are conducted. As shown in Fig. 7d, the piezoelectric charges of 17 recycling experiments are almost keeping stable, demonstrating the good stability and cyclicity of PVDF/CI films as a magnetic field sensor. Therefore, PVDF/CI magnetic films possess ideal magnetic-mechanic-electric coupling properties under the loading of magnetic field and exhibit broad potential in sensing the magnetic field.

3.6. The mechanism of magnetic-mechanic-electric coupling properties

In this work, the combination of CI particles and PVDF matrix together is important for the generation of magneto-electric effect (Fig. 8). PVDF is a typical piezoelectric material, which responds to the external deformation or force by generating piezoelectric signals. This positive piezoelectric effect enables PVDF matrix to be widely applied in sensor area [30–33]. For PVDF/CI composites, the electrical signals will be generated under the action of magnetic force due to the magnetic-mechanic-electric coupling effect in piezoelectric film. Here, the mechanism of magnetoelectric behavior can be explained from two aspects.

Firstly, under applying an external magnetic field, the magnetic CI particle is magnetized. The induced magnetic dipole forced the CI particles to move together. The CI particles are located within the PVDF matrix, thus they will squeez the PVDF matrix, resulting a magnetostrictive effect. To this end, the PVDF/CI composite is strengthened under the magnetic field. The magnetic dipole-dipole forces act on the PVDF/CI composite and thus leads to the generation of piezoelectric charges. Without the magnetic field, no magnetostrictive effect is found in the composite. Then, the PVDF/CI composite is magnetic, which is originated from the CI particles, thus it is active to the external magnetic field. Under applying the magnetic field, the induced magnetic-dipole in CI particles forces the film toward the magnetic field. This magnetic force leads to the bending of PVDF/CI film along the magnetic field, which further induces the formation of piezoelectric charges. Finally, the upper and lower surfaces of the piezoelectric film will produce equal amounts of induced-charges with opposite polarity along the PVDF molecular chain [26]. As a result, PVDF/CI composite is sensitive to the magnetic field and the piezoelectric charges increase with the magnetic field strength, thus PVDF/CI composite can be applied in both of the magnetic field and deformation sensor.

4. Conclusion

In this work, a multi-functional magneto-electric PVDF/CI composite film with distinct piezoelectric effect and magneto-electric effect is reported by doping magnetic CI particles into piezoelectric PVDF matrix. The unilateral bending experiments show that PVDF/CI film is sensitive to the deformation, thus the piezoelectric charge signals are dependent on the bending displacement. The large deformation leads to more piezoelectric charges, exhibiting the positive piezoelectric effect. Interestingly, the piezoelectric effect of PVDF/CI films is controlled by the external magnetic field. With increasing of the magnetic field loading, the amount of piezoelectric charges also simultaneously increases, indicating obvious magneto-electric properties. The quantitative relationship between magnetic field and magneto-electric charges was eventually obtained. Because PVDF/CI film is sensitive to both the magnetic field and deformation, it is expected to be an ideal candidate for smart sensors. The further work on developing its application in sensor area is advancing.

Acknowledgements

Financial supports from the National Natural Science Foundation of China (Grant Nos. 11572309 & 11572310) are gratefully acknowledged. This work was also supported by the Strategic Priority Research Program of the Chinese Academy of Sciences (Grant No. XDB22040502), the Fundamental Research Funds for the Central Universities (WK2480000002), and Collaborative Innovation Center of Suzhou Nano Science and Technology.

Appendix A. Supplementary data

Supplementary data related to this article can be found at http://dx.doi.org/10.1016/j.compscitech.2018.06.006.

References

[1] M. Alnassar, A. Alfadhel, Y.P. Ivanov, J. Kosel, Magnetoelectric polymer nanocomposite for flexible electronics, J. Appl. Phys. 117 (17) (2015) 17D711.
[2] R. Gonçalves, A. Larrea, M.S. Sebastian, V. Sebastian, P. Martins, S. Lanceros-Mendez, Synthesis and size dependent magnetostrictive response of ferrite nanoparticles and their application in magnetoelectric polymer-based multiferroic sensors, J. Mater. Chem. C 4 (45) (2016) 10701–10706.
[3] D. Chen, H. Quan, Z. Huang, S. Luo, X. Luo, F. Deng, H. Jiang, G. Zeng, Electromagnetic and microwave absorbing properties of RGO@hematite core–shell

nanostructure/PVDF composites, Compos. Sci. Technol. 102 (2014) 126–131.
[4] X.J. Zhang, G.S. Wang, W.Q. Cao, Y.Z. Wei, J.F. Liang, L. Guo, M.S. Cao, Enhanced microwave absorption property of reduced graphene oxide (RGO)-$MnFe_2O_4$ nanocomposites and polyvinylidene fluoride, ACS Appl. Mater. Interfaces 6 (10) (2014) 7471–7478.
[5] R. Gupta, M. Tomar, A. Kumar, V. Gupta, Performance of magnetoelectric PZT/Ni multiferroic system for energy harvesting application, Smart Mater. Struct. 26 (3) (2017) 035002.
[6] X. Huo, W. Li, J. Zhu, L. Li, Y. Li, L. Luo, Y. Zhu, Composite based on Fe_3O_4@$BaTiO_3$ particles and polyvinylidene fluoride with excellent dielectric properties and high energy density, J. Phys. Chem. C 119 (46) (2015) 25786–25791.
[7] S.S. Hossain, P.K. Roy, Structural and electro-magnetic properties of low temperature co-fired $BaSrTiO_3$ and NiCuZn ferrite composites for EMI filter applications, J. Mater. Sci. Mater. Electron. 28 (23) (2017) 18136–18144.
[8] R. Kumaran, S.D. Kumar, N. Balasubramanian, M. Alagar, V. Subramanian, K. Dinakaran, Enhanced electromagnetic interference shielding in a Au–MWCNT composite nanostructure dispersed PVDF thin films, J. Phys. Chem. C 120 (25) (2016) 13771–13778.
[9] M. Fiebig, Revival of the magnetoelectric effect, J. Phys. D Appl. Phys. 38 (8) (2005) 123–152.
[10] M. Stingaciu, P.G. Reuvekamp, C.W. Tai, R.K. Kremer, M. Johnsson, The magnetodielectric effect in $BaTiO_3$–$SrFe_{12}O_{19}$ nanocomposites, J. Mater. Chem. C 2 (2) (2014) 325–330.
[11] A. Goshkoderia, S. Rudykh, Stability of magnetoactive composites with periodic microstructures undergoing finite strains in the presence of a magnetic field, Compos. B Eng. 128 (2017) 19–29.
[12] S. Rudykh, K. Bertoldi, Stability of anisotropic magnetorheological elastomers in finite deformations: a micromechanical approach, J. Mech. Phys. Solid. 61 (2013) 949–967.
[13] S. Jiang, H. Wan, H. Liu, Y. Zeng, J. Liu, Y. Wu, G. Zhang, High β phase content in PVDF/$CoFe_2O_4$ nanocomposites induced by DC magnetic fields, Appl. Phys. Lett. 109 (10) (2016) 102904.
[14] M.M. Abolhasani, K. Shirvanimoghaddam, M. Naebe, PVDF/graphene composite nanofibers with enhanced piezoelectric performance for development of robust nanogenerators, Compos. Sci. Technol. 138 (2017) 49–56.
[15] J. Guan, C. Xing, Y. Wang, Y. Li, J. Li, Poly (vinylidene fluoride) dielectric composites with both ionic nanoclusters and well dispersed graphene oxide, Compos. Sci. Technol. 138 (2017) 98–105.
[16] J.A. Puértolas, J.F. García-García, F.J. Pascual, J.M. González-Domínguez, M.T. Martínez, A. Ansón-Casaos, Dielectric behavior and electrical conductivity of PVDF filled with functionalized single-walled carbon nanotubes, Compos. Sci. Technol. 152 (2017) 263–274.
[17] L. Ren, J. Zhao, S. Wang, J. Zha, G. Hu, Z. Dang, Remarkably variable dielectric and magnetic properties of poly(vinylidene fluoride) nanocomposite films with triple-layer structure, Compos. Sci. Technol. 107 (2015) 107–112.
[18] H.H. Singh, S. Singh, N. Khare, Design of flexible PVDF/$NaNbO_3$/RGO nanogenerator and understanding the role of nanofillers in the output voltage signal, Compos. Sci. Technol. 149 (2017) 127–133.
[19] Z. Wang, T. Wang, M. Fang, C. Wang, Y. Xiao, Y. Pu, Enhancement of dielectric and electrical properties in BFN/Ni/PVDF three-phase composites, Compos. Sci. Technol. 146 (2017) 139–146.
[20] W. Jing, F. Fang, A flexible multiferroic composite with high self-biased magnetoelectric coupling, Compos. Sci. Technol. 153 (2017) 145–150.
[21] T.I. Becker, K. Zimmermann, D.Y. Borin, G.V. Stepanov, P.A. Storozhenko, Dynamic response of a sensor element made of magnetic hybrid elastomer with controllable properties, J. Magn. Magn. Mater. 449 (2018) 77–82.
[22] L. Ding, S. Xuan, J. Feng, X. Gong, Magnetic/conductive composite fibre: a multifunctional strain sensor with magnetically driven property, Composer Part A-Appl. S 100 (2017) 97–105.
[23] S. Reis, M.P. Silva, N. Castro, V. Correia, J. Gutierrez, A. Lasheras, S. Lanceros-Mendez, P. Martins, Optimized anisotropic magnetoelectric response of $Fe_{61.6}Co_{16.4}Si_{10.8}B_{11.2}$/PVDF/$Fe_{61.6}Co_{16.4}Si_{10.8}B_{11.2}$ laminates for AC/DC magnetic field sensing, Smart Mater. Struct. 25 (5) (2016) 055050.
[24] D. Min, W. Zhou, F. Luo, D. Zhu, Facile preparation and enhanced microwave absorption properties of flake carbonyl iron/Fe_3O_4 composite, J. Magn. Magn. Mater. 435 (2017) 26–32.
[25] Y. Qing, D. Min, Y. Zhou, F. Luo, W. Zhou, Graphene nanosheet- and flake carbonyl iron particle-filled epoxy–silicone composites as thin–thickness and wide-bandwidth microwave absorber, Carbon 86 (2015) 98–107.
[26] J. Feng, S. Xuan, L. Ding, X. Gong, Magnetoactive elastomer/PVDF composite film based magnetically controllable actuator with real-time deformation feedback property, Composer Part A-Appl. S 103 (2017) 25–34.
[27] R. Gonçalves, P. Martins, D.M. Correia, V. Sencadas, J.L. Vilas, L.M. León, G. Botelho, S. Lanceros-M´endez, Development of magnetoelectric $CoFe_2O_4$/poly (vinylidene fluoride) microspheres, RSC Adv. 5 (45) (2015) 35852–35857.
[28] Y.Q. Fu, J.K. Luo, N.T. Nguyen, A.J. Walton, A.J. Flewitt, X.T. Zu, Y. Li, G. McHale, A. Matthews, E. Iborra, H. Du, W.I. Milne, Advances in piezoelectric thin films for acoustic biosensors, acoustofluidics and lab-on-chip applications, Prog. Mater. Sci. 89 (2017) 31–91.
[29] M. Pohanka, The piezoelectric biosensors: principles and applications, a review, Int. J. Electrochem. Sci. 12 (2017) 496–506.
[30] S. Garain, S. Jana, T.K. Sinha, D. Mandal, Design of in situ poled Ce(3+)-Doped electrospun PVDF/graphene composite nanofibers for fabrication of nanopressure sensor and ultrasensitive acoustic nanogenerator, ACS Appl. Mater. Interfaces 8 (7) (2016) 4532–4540.
[31] Z. Liu, X. Yang, J. Sun, F. Ma, PVDF modified Pd-SnO_2 hydrogen sensor with stable response under high humidity, Mater. Lett. 212 (2018) 283–286.
[32] S.M. Hosseini, A.A. Yousefi, Piezoelectric sensor based on electrospun PVDF-MWCNT-Cloisite 30B hybrid nanocomposites, Org. Electron. 50 (2017) 121–129.
[33] Y.J. Yang, S. Aziz, S.M. Mehdi, M. Sajid, S. Jagadeesan, K.H. Choi, Highly sensitive flexible human motion sensor based on $ZnSnO_3$/PVDF composite, J. Electron. Mater. 46 (7) (2017) 4172–4179.